Int. J. Bio-Inorg. Hybr. Nanomater., 5(1): 61-71, Spring 2016

Adsorption destructive study of Chlorpyrifos (CP) on the Nickel Tungstate ($NiWO_4$) nanoparticles catalyst by ^{31}PNMR

M. Sadeghi[1]; S. Yekta[2]; H.Ghaedi[3]*

[1]*Young Researchers and Elite Club, Ahvaz Branch, Islamic Azad University, Ahvaz, Iran*
[2]*Department of Chemistry, Faculty of Basic Sciences, Islamic Azad University, Qaemshahr Branch, Qaemshahr, Iran*
[3]*Faculty of Engineering, Bushehr Branch, Islamic Azad University, Bushehr, Iran*

Received: 25 January 2016; Accepted: 28 March 2016

ABSTRACT: In this research, the adsorption destructive process of chlorpyrifos (CP,O,O-Diethyl-O-3,5,6-trichloro-2-pyridinyl phosphorothioate) as a noticeable organophosphate pesticide using in agriculture on the nickel tungstate ($NiWO_4$) nanoparticles catalyst was investigated and monitored via the ^{31}P nuclear magnetic resonance (^{31}PNMR). The effects of various experimental parameters such as catalyst dosage, contact time, initial chlorpyrifos concentration and temperature on the elimination efficiency of chlorpyrifos were surveyed. Nickel tungstate ($NiWO_4$) nanoparticles were synthesized by hydrothermal method using $NiCl_2$ and Na_2WO_4 as the precursors and source of Ni and W, respectively. The structural, morphological, crystal size and elemental composition of the pre-prepared nanoparticles powder were identified using Scanning electron microscopy-energy dispersive micro-analysis (SEM-EDAX), X-ray diffraction (XRD) and Fourier transform infrared (FTIR) techniques. ^{31}PNMR results indicated that chlorpyrifos was successfully eliminated by the catalyst with a yield 100% under optimized conditions. The parameters including: contact time (300 min), catalyst dose (0.3 g/L), initial pesticide concentration (5 mg/L) and temperature (298°K) were considered as optimized conditions for this process. Besides, the reaction kinetic information was studied by applying first order model. The values of the rate constant (k) and half-life ($t_{1/2}$) were determined as 0.0037 1/min and 187.2972 min, respectively. The main product resulted from destruction reaction between chlorpyrifos and $NiWO_4$ is diethyl phosphorothioic acid (DEPA) which is less toxic than primary pesticide.

Keywords: *Adsorption destructive; DEPA; Kinetic; $NiWO_4$ nanoparticles; ^{31}PNMR*

INTRODUCTION

In recent years, the concerns about different sorts of toxicants originated from human corresponded activities and their undesirable entrance to the environment have been raised progressively. The massive utilization of variant pesticides in agricultural fields and the subsequent inopportune storage and disposal of scum pesticides are considered as a major origin of contamination of soil, ground water, rivers, lakes, rain water and air (Samet, *et al.,* 2010). Chlorpyrifos (CP,O,O-Diethyl-O-3,5,6-trichloro-2-pyridinyl phosphorothioate) is one of the most applied organophosphate in agriculture. Also, it should be noted that the intuitive toxic characteristics of these pesticides prevail the

(*) Corresponding Author - e-mail: sina.yekta.chem@gmail.com

agricultural insect pests. It was reported that the annual average global utilization of chlorpyrifos containing pesticides between 2002 and 2006 was estimated 25 million kg active ingredient and 98.5% of this mentioned amount was exerted for agricultural goals. The extreme and heedless use of chlopyrifos in many countries has already caused serious environmental contamination and recognized as an imminent threat for human being and environment. Plus, it is notable that chlorpyrifos insecticide has been found in marine, sediment, sumps, streams, rivers, sloughs, fresh water, urban storm drains, ground water, fog and air as hinted above (Whitacre, 2012). The chemical structure and physicochemical of chlorpyrifos has been represented in Table 1. Moreover, chlorpyrifos remains biologically active in soil for time periods ranging from 20 to 90 days and also is nearly indelible, with variable half-life from 10 to 60 days (Getzin, 1981, Lakshmi, *et al.,* 2008). The specified half-life range depends on the fact that the degradation of chlorpyrifos in soil is related to its initial concentration, soil moisture, temperature and pH (Racke, *et al.,* 1994, Awasthi and Prakash 1997). By considering the deleterious perspective of chlorpyrifos, its use has been vastly confined in the United States of America (U.S.A) and some European countries, even for agricultural goals. However, this insecticide is still in use in about 100 of other counties. Similar to other organophosphorous pesticides, chlorpyrifos suppresses the cholinesterase, enzyme systems indispensable for the normal function of nervous system. The most commonly reported effects of chlorpyrifos poisoning include: headache, dizziness, nausea, blurred vision, excess sweating, salivation, muscle weakness, abdominal cramps, and diarrhea and in some extreme cases even leads to death (Cochran, 2002). Nowadays, different innovative and beneficial techniques have been developed for waste water treatment containing chlopyrifos. These include the use of the photocatalytic degradation using TiO_2 as catalyst (Penuela and Barcelo, 1997), ultra sonic irradiation (Zhang, *et al.,* 2011), ionizing radiation (Mori, 2006), high-pressure arc discharge plasma process (Meiqiang, *et al.,* 2006), electrochemical degradation (Samet, *et al.,* 2010), photo-Fenton process (Bavcon Kralj, *et al.,* 2007), chemical oxidation using hypochlorous acid (HOCl) as the primary oxidant (Stephen and Timothy, 2006), the use of ozone (O_3) (Whangchai, *et al.,* 2011) and hydrolysis (Benoit-Marqui, *et al.,* 2004). Furthermore, many studies have shown that the dissolved metal ions can affect the catalysis of organophosphorous pesticides positively and have significant role in the catalysis process. According to the above discussed issue, in most cases, the catalytic enhancement is surely attributed to metal coordination with the substrate (Sarkouhi, *et al.,* 2016). Recently, the reports have revealed that there is a great interest using solid sorbent decontaminants such as nano metal oxides in wide variant scientific fields. Several nano-crystalline metal oxides like ZrO_2 (Verma, *et al.,* 2016), CuO (Verma, *et al.,* 2015), MnO_2 (Verma, *et al.,* 2016) and ZnO-CdO (Sadeghi and Yekta 2014) have been synthesized as effective adsorbents and catalysts using in wide scope of researches (Singh, *et al.,* 2011). Also inorganic structures associated with nano-sized dimensions and morphological quality has gained a great tendency due to the low density and high specific surface area of these nano-structures materials (Sarkouhi, *et al.,* 2016). Nickel tungstate as a substantial inorganic salt belongs to metal tungstate clan. Besides, $NiWO_4$ has a desirable potential for application in various fields of industries such as catalysts (Stern and Grasselli, 1997) and humidity sensors (Sundaram and Nagaraja, 2004) due to its attractive catalytic activity and suitable sensitivity to humidity. Further, $NiWO_4$ could be applied extensively in other fields like microwave devices (Pullar, *et al.,* 2007), microwave applications (Johnson, *et al.,* 1962), optical fibers (Wang, *et al.,* 1992), scintillator materials (Carel and van Eijk, 1997) and photoanodes (Pandey, *et al.,* 2006). Meantime, metal tungstate compounds are utilized as photocatalyst for removal of several organic pollutants namely organic dyes from water media (He, *et al.,* 2010). Lately, $NiWO_4$ nano particles have attracted much attention because of their large surface area and noticeable quantum size effect which cause better photocatalytic activity (Pandey, *et al.,* 2006). Plus, there are different methods for synthesis of nano-sized $NiWO_4$ catalysts with several morphologies containing: molten salt method (Song, *et al.,* 2009), modified citrate complex technique (Ryu, *et al.,* 2006) co- precipitation (Quintana-Melgoza, *et al.,* 2001), spray pyrolysis (Pullar, *et al.,* 2007), poly-

Table 1: Chemical structure and physicochemical of chlorpyrifos (CP).

Structure	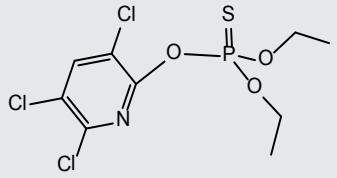
Chemical formula	$C_9H_{11}Cl_3NO_3PS$
Density (g/cm^3)	1.398
Molar mass (g/mol)	350.50
Melting point (°C)	43
Boiling point (°C)	160

meric precursor method (De Oliveira, *et al.,* 2009) and hydrothermal method (Dias and Ciminelli, 2001). In this work, the $NiWO_4$ nano particles were synthesized by hydrothermal method as one of the most applying methods for the adsorption-destruction of chlorpyrifos. Also, there are no papers reporting the application of $NiWO_4$ catalyst used to eliminate this pesticide.

EXPERIMENTAL SECTION

Materials and reagents

The materials including: Nickel chloride hexahydrate ($NiCl_2.6H_2O$) (98%, Sigma Aldrich), sodium tungstate dihydrate ($Na2WO_4.2H_2O$) (99%, Sigma Aldrich), chlorpyrifos (CP,O,O-Diethyl-O-3,5,6-trichloro-2-pyridinyl phosphorothioate) (98%, Sigma Aldrich), phosphoric acid (85%, Merck), octane (98%, Merck) and chloroform-d ($CDCl_3$) (99.8%, Sigma Aldrich) were used as received and without further purification for the synthesis of $NiWO_4$ nanoparticles. Further, the high purified water was used during all synthesis procedures where was in need.

Instrumentation

The synthesized nanoparticles were undergone characterization by different well known techniques. The morphology, particle sizes and elemental composition of the prepared adsorbents were studied using a scanning electron microscope (SEM, HITACHI S-300N). Moreover, an energy-dispersive x-ray spectrometer (EDAX) connected to LEO-1530VP XL30 Philips scanning electron microscope was applied for semi-quantative analysis. Also, the crystallographic characteristics of the synthesized $NiWO_4$ nanoparticles were perused by X-ray diffraction analysis recorded with a Philips X'pert MPD system using Cu Ka X-ray radiations (k = 1.54056 A°). Data were collected over the scope of 4–80° in 2θ with a scanning speed of 2° min^{-1}. The IR spectra were scanned on a PerkinElmer model 2000 FTIR spectrometer (USA) in the wavelength range of 400 to 4000 cm^{-1} using KBr pellets. Phosphorous-31 Nuclear Magnetic Resonance (NMR) spectra were recorded on Bruker DPX-250 spectrometer producing 250 MHz Radio Frequency (RF) and centrifuge (Universal, CAT. NO. 1004) instrument was exerted.

Synthesis procedure of the $NiWO_4$

The $NiWO_4$ nanoparticles were synthesized via hydrothermal method (Mani, *et al.,* 2016). 0.001 mol of sodium tungstate dihydrate ($Na_2WO_4.2H_2O$) was added and dissolved in 25 mL of distilled water and the mixture solution was agitated by ultrasonic for 10 min. Next, 0.001 mol of nickel chloride hexahydrate ($NiCl_2.6H_2O$) was added to the above prepared solution and then the system was undergone rigorous stirring until complete dissolution of all powders. Then, the solution was transferred into a 40 mL Teflon-lined stainless steel autoclave maintaining at 180°C for 5 h and eventually cooled to room temperature. At last, the light green precipitates were gained and washed subsequently for five times with high purified water and ethanol. The final solid powder product was then dried at 50°C overnight and calcined in sequence at 600°C for 4h. Eq. (1) in below represents the main reaction taking place during the synthesis of $NiWO_4$ nanoparticles.

$$NiCl_2.6H_2O + Na_2WO_4.2H_2O \rightarrow NiWO_4 + 2NaCl + 8H_2O \quad (1)$$

Reaction procedure of chlorpyrifos on the $NiWO_4$

The sample preparation procedure contains four major steps: first, 0.05 mL of phosphoric acid (H_3PO_4) diluted with 25 mL of deionized water reaching 0.03 M H_3PO_4 as the blank solution. Afterwards, this blank solution was injected to a capillary column with closed tips by heat (S1). Second step, corresponded to the preparation of chlorpyrifos solutions by addi-

tion of 5, 10, 20, 30, 40 and 50 mg/L of chlorpyrifos pesticide to 10 mL of a 1:1 (v/v) ratio of octane: water as the solvent (S2). At third step, the S2 prepared solutions were all mixed separately with 0.1, 0.2, 0.3, 0.4 and 0.5 g of $NiWO_4$ nanoparticles in five 50 mL Erlenmeyer flasks and stirred intensely for 8h at 298-328°K (S3). At fourth step, 1 mL of each of pre-prepared S3 mixtures was posed in centrifuge tubes and centrifuged at 500 rpm for 4 min. Then, 0.3 mL of the above mentioned samples and 0.1 mL of chloroform-d ($CDCl_3$) were added to NMR tubes associated with the capillary column (S1 solution) as the blank solution. Eventually, the ^{31}PNMR analysis was exerted for measuring the amount of pesticide in a sample.

RESULTS AND DISCUSSION

SEM-EDAX analysis

The SEM images were used for investigation of morphologies and crystalline sizes of synthesized nanoparticles. Fig. 1 demonstrates the SEM of $NiWO_4$ nanoparticles synthesized with different magnifications. The homogeneous morphology of $NiWO_4$ nanoparticles and their primary size estimation (under the 100 nm) could be explicitly revealed by SEM images. Fig. 2 shows the EDAX spectrum for synthesized $NiWO_4$ nanoparticles. The peaks of the EDAX pattern corroborate that the final product is highly pure, and desirable quantities (the average atomic percent-

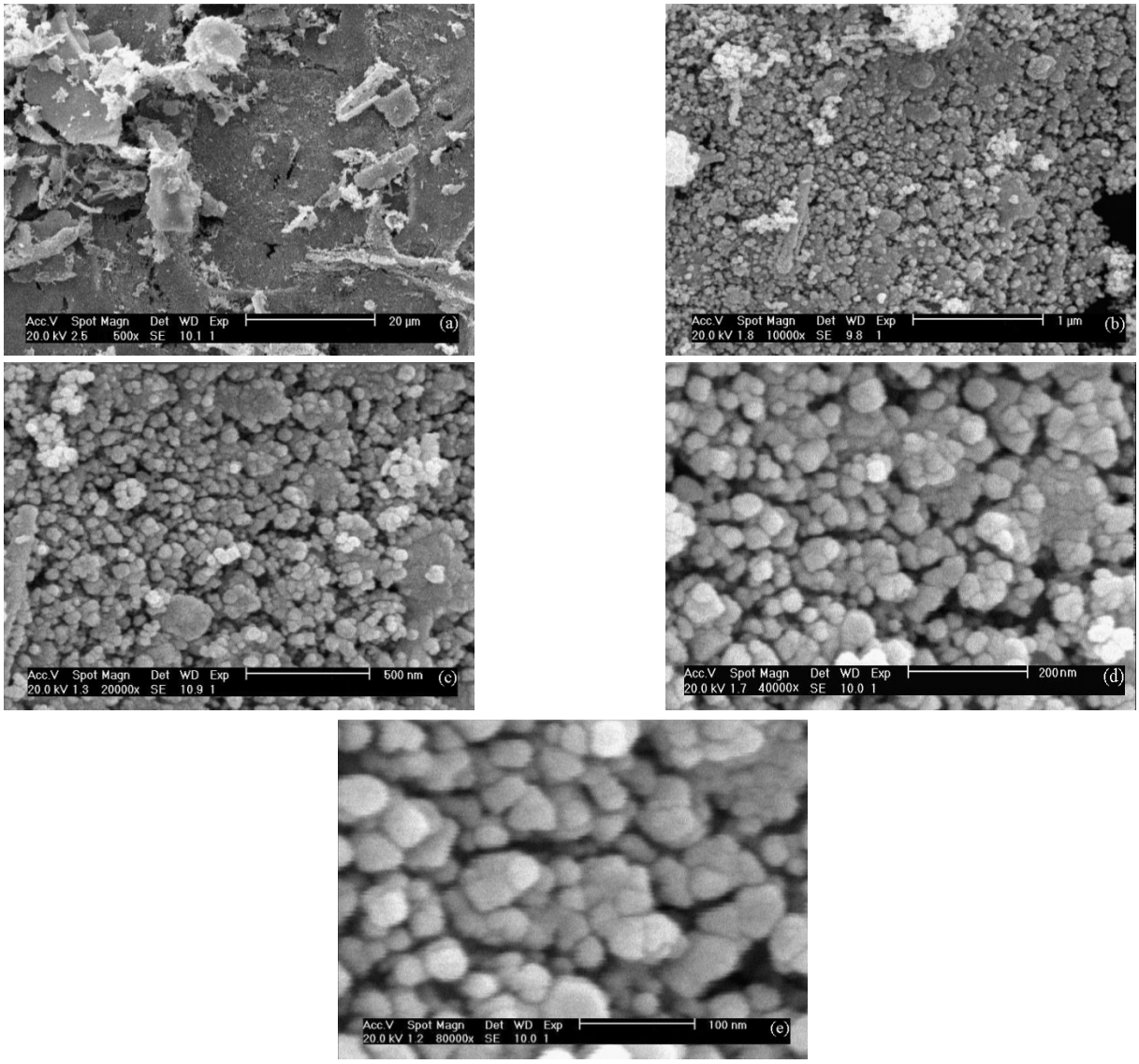

Fig. 1: SEM images of $NiWO_4$ nanoparticles with different magnifications (500 to 80000 x).

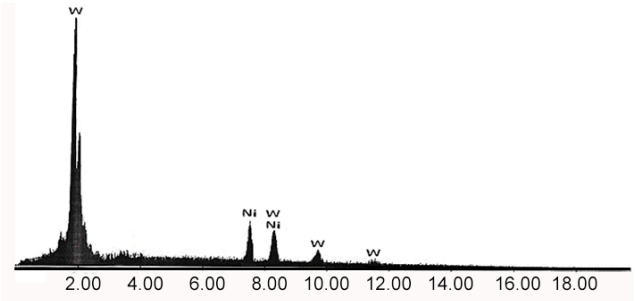

Fig. 2: EDAX analysis of $NiWO_4$ nanoparticles.

age) of W and Ni elements in the synthesized sample are 76.48% and 23.52%, respectively. This elemental analysis clarifies the existence of corresponding elements in their stoichiometric percentage.

XRD patterns

Fig. 3 represents the XRD pattern related to the synthesized nickel tungstate nanoparticles. The observed diffraction peaks were well matched with Joint Committee for Powder Diffraction Standards (JCPDS No. 15-0755). There are different narrow peaks for $NiWO_4$ showing the crystalline nature of the synthesized nanoparticle. The obtained diffraction peaks are affiliated to planes (010), (100), (011), (110), (111), (002), (200), (121), (112), (211), (022), (220), (130), (202), (113) and (311), respectively. Plus, no peak corresponded to any impurity was observed in the XRD pattern. The crystalline size of the prepared sample was calculated using Scherrer formula (2):

$$d = \frac{0.94\lambda}{\beta \cos\theta} \qquad (2)$$

Where d is the crystalline size, λ is the wavelength of X-ray Cu Kα source (equal 1.54056 Å), β is corresponded to the full width at half maximum (FWHM)

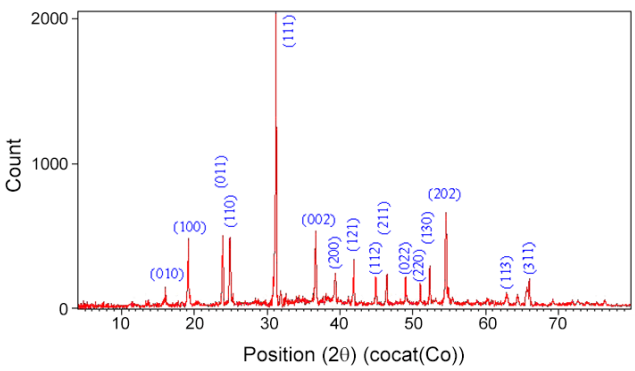

Fig. 3: XRD patterns of $NiWO_4$ nanoparticles.

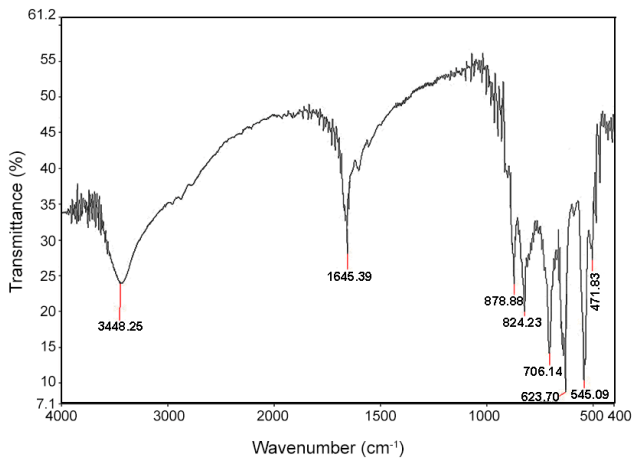

Fig. 4: FTIR spectrum of $NiWO_4$ nanoparticles.

of the most predominant peak at 100 % intensity and θ is Bragg diffraction angle at which the peak is recorded. Using this formula, the smaller average particle sizes by Debye-Scherrer formula were estimated to be 26.8 nm.

FTIR spectrum

The formation of $NiWO_4$ and presence of the corresponding functional groups were also proved by FTIR spectroscopy. The FTIR spectrum of the synthesized $NiWO_4$ is revealed in Fig. 4. As can be observed from spectrum, the peaks at 3448 and 1645 cm^{-1} are affiliated to the stretching and bending vibrations of O–H and H–O–H of the water molecules that are absorbed on the surface of the sample. Though, six absorption bands (878, 824, 706, 623, 545 and 471 cm^{-1}) were perceived in the spectrum of the annealed wolframic sample. Also, the absorption bands occurred at 878 and 824 cm^{-1} were considered to be owing to the vibration of the WO_2 units in the W_2O_8 groups. The absorption bands at 706 and 623 cm^{-1} are a class of a two-oxygen bridge (W_2O_2) and related to the asymmetric stretching of the same units. The observed absorptions in the range of 545 and 471 cm^{-1} are owing to the vibrations of the NiO_6 polyhedral. Therefore, the occurred peaks in the spectrum for the annealed sample verify the formation of crystalline $NiWO_4$ nanoparticles.

^{31}PNMR analysis

The adsorption-destruction (elimination) reactions of chlorpyrifos (CP) on the $NiWO_4$ nanoparticles were investigated under various experimental condisions

and octane solvent using ^{31}P nuclear magnetic resonance ($^{31}PNMR$) technique. Furthermore, the quantitative actions of $^{31}PNMR$ spectroscopy were fulfilled in the presence of phosphoric acid (H_3PO_4) as an appropriate inorganic internal standard for the measurment of reaction efficiency. Afterwards, the proportion of chlorpyrifos integral to H_3PO_4 (chlorpyrifos integral/ H_3PO_4 integral) was considered and calculated. From the spectra, three signals were revealed. Two narrow peaks at approximately δ= 60 and 41 ppm affiliated to the chemical shifts of chlorpyrifos and diethyl phosphorothioic acid (DEPA) respectively, and the characteristic sharp peak at near δ= 0 (zero) ppm also corresponded to the phosphoric acid (H_3PO_4).

Effect of contact time

To investigate the effect of time on the elimination procedure of chlorpyrifos on the $NiWO_4$ nanoparticles, different time intervals was considered for experiments to be carried out. These series of experiments assemble a logical comparison between elimination ability of adsorbent and time intervals. Fig. 5 shows the variation of elimination rate (%) against shaking time and also the reliability of elimination yield of chlorpyrifos on the $NiWO_4$ nanoparticles to the contact time. The elimination time was surveyed in the range of 0-300 min. Thus, to achieve a suitable reaction time, 300 min was selected as an optimum value. $^{31}PNMR$ spectra and data results are depicted in Fig. 6 and Table 2.

Effect of catalyst dose

The designation of optimized dosage of a catalyst is of great significance in any type of scientific analytical research because one of the key parameters that makes a new adsorbent remarkable and also reliable is to use

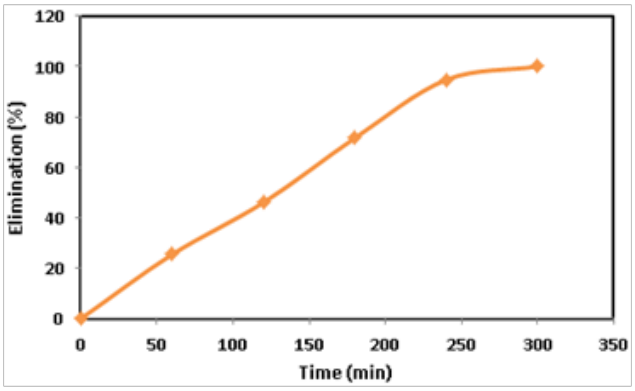

Fig. 5: Effect of contact time on the elimination of chlorpyrifos by $NiWO_4$ nanoparticles (optimum conditions: initial concentration= 5 mg/L, catalyst dosage= 0.3 g/L, T= 298°K).

the least dose of it for the most value of elimination. In present research, to designate the optimized catalyst dose for the elimination of chlorpyrifos, the elimination characteristics of chlorpyrifos was explored at range of 0.05-0.5 g of $NiWO_4$ nanoparticles. As explained in Fig. 7, the more the dose of adsorbent, the better the destruction efficiency, until the point after which no more sensible variations is observed and the curve slope tend to a linear form which implies constant values. Finally, the value of 0.3 g was considered as the effective dose for $NiWO_4$ nanoparticles to perform high yield adsorption- destruction process.

Effect of initial concentration of chlorpyrifos

The effect of initial concentration of chlorpyrifos in the range of 5 to 50 mg/L on elimination was studied and is depicted in Fig. 8. From the Figure, it is obvious that the percentage of chlorpyrifos elimination decreased with the consecutive increase in initial concentration of chlorpyrifos owing to the fixed quantity of adsorbents used in this research. The initial concentration of chlorpyrifos assembles the intransitive driving force to

Table 2: $^{31}PNMR$ spectra results for CP-$NiWO_4$ samples under optimum conditions: initial concentration= 5 mg/L, catalyst dosage= 0.3 g/L, T= 298°K

Sample	Time (min)	H_3PO_4 Intg	CP Intg	CP Intg/ H_3PO_4 Intg	DEPA Intg
a	0	1.0000	4.0299	4.0299	0.0000
b	60	1.0000	3.0050	3.0050	0.4490
c	120	1.0000	2.1740	2.1740	1.2390
d	180	1.0000	1.1450	1.1450	2.2490
e	240	1.0000	0.2126	0.2126	3.1738
f	300	1.0000	0.0000	0.0000	3.5540

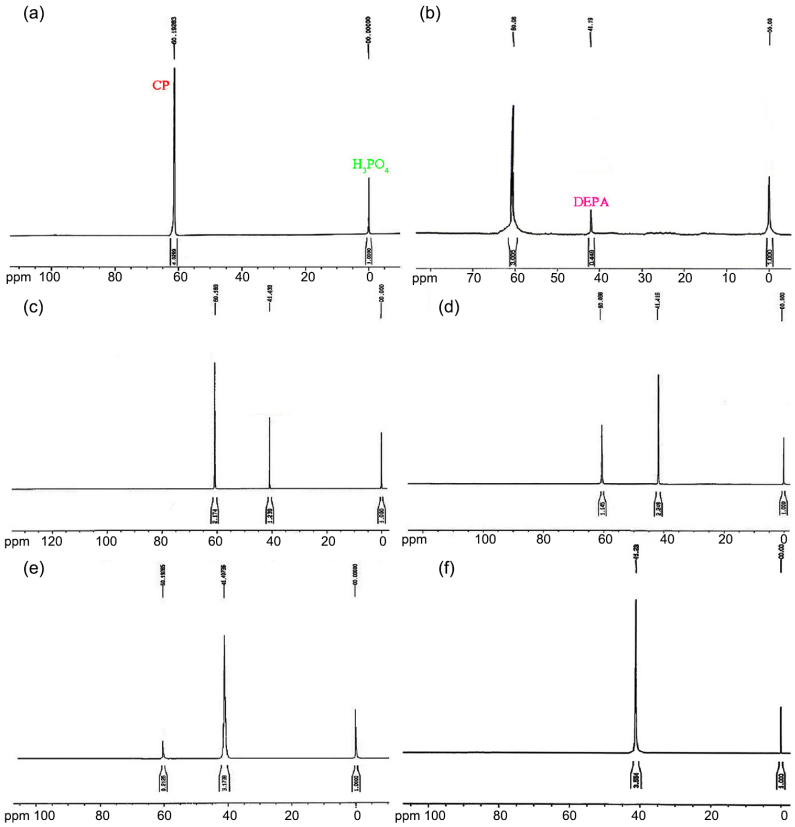

Fig. 6: ^{31}PNMR spectra of CP-$NiWO_4$ nanoparticles sample; the following structural assignments were made at (a) δ= 60 ppm (CP), (b) δ= 41 ppm (DEPA) and (c) δ= 0 ppm, (H_3PO_4), at different interval times, a) 0, b) 60, c) 120, d) 180, e) 240 and f) 300 min, (optimum conditions: catalyst dosage= 0.3 g/L, initial concentration= 5 mg/L, T= 298°K).

conquer the resistance to the mass transfer of chlorpyrifos between the aqueous phase and the solid phase. The enhancement in initial concentration of chlorpyrifos also increases the interaction between chlorpyrifos and $NiWO_4$ nanoparticles. Thereupon, an increase in initial concentration of chlorpyrifos enhances the elimination of chlorpyrifos but as mentioned above the fixed amount of adsorbent with particular capacity confines the adsorption and after a while the elimination percentage descends as a result. The maximum percentage chlorpyrifos elimination was found to be

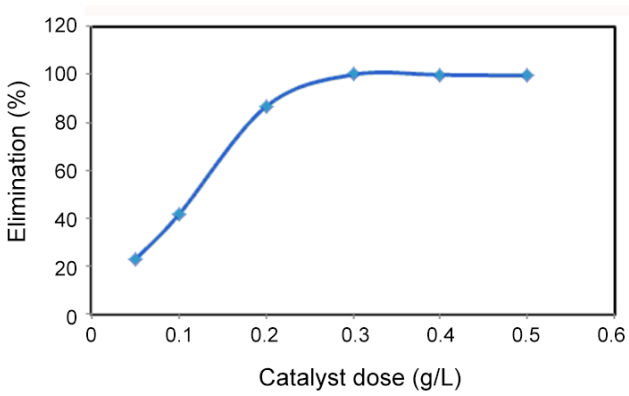

Fig. 7: Effect of catalyst dose on the elimination of chlorpyrifos by $NiWO_4$ nanoparticles (optimum conditions: initial concentration = 5 mg/L, contact time= 300 min, T= 298°K).

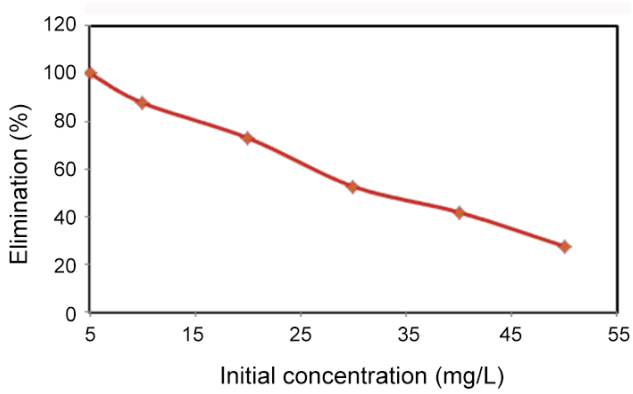

Fig. 8: Effect of initial chlorpyrifos concentration on the elimination of chlorpyrifos by $NiWO_4$ nanoparticles (optimum conditions: catalyst dosage= 0.3 g/L, contact time= 300 min, T= 298°K).

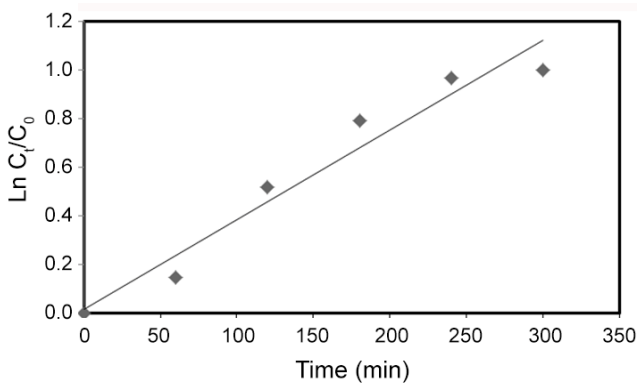

Fig. 9: Plot of Ln C_t/C_o versus time (optimum conditions: initial concentration = 5 mg/L, catalyst dosage= 0.3 g/L, T= 298°K).

100% for 5 mg/L of initial concentration.

Determination of kinetics parameters

In order to determine the elimination kinetics, plots of Ln (concentration) versus reaction time were made (Fig. 9). The elimination rate constant (slope), k, was calculated from the first order equation: $C_t = C_o e–kt$ where C_t is related to the concentration of the chlorpyrifos at time t, C_o is corresponded to the initial concentration and k is the elimination rate constant. Besides, the half-life ($t_{1/2}$) can be specified by $t_{1/2}$= Ln2/k. Further, the samples for adsorption kinetics investigation were provided by adding 0.3 g of $NiWO_4$ nanoparticles into the separate containers containing 5 mg/L of chlorpyrifos, at 298 K, and certain time intervals. The results have been represented in Table 3.

Table 3: First order kinetic parameters for the elimination of chlorpyrifos by $NiWO_4$ nanoparticles under optimum conditions: initial concentration= 5 mg/L, catalyst dosage= 0.3 g/L, T= 298°K.

Kinetic equation	k (1/min)	$t_{1/2}$ (min)	R^2
y= 0.0037x+0.0193	0.0037	187.2972	0.9516

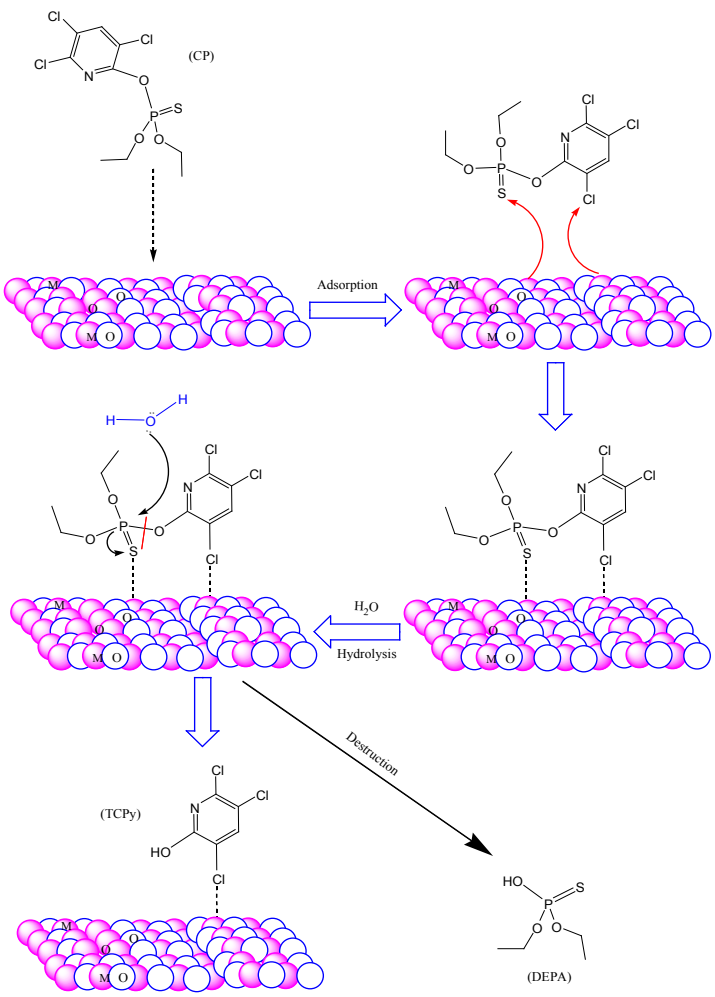

Scheme 1: Reaction pathway proposed for the CP elimination on the NiWO4 nanoparticles (M= Ni or/and W)

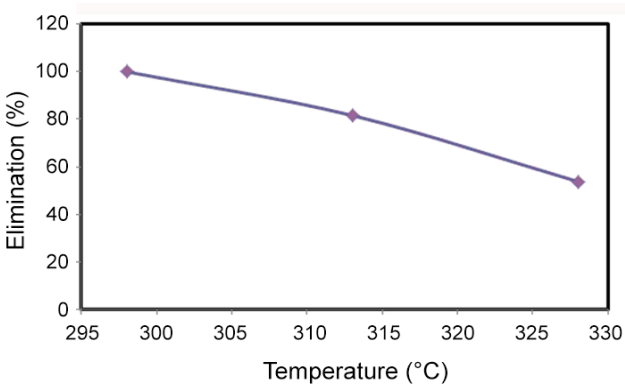

Fig. 10: Plot of chlorpyrifos elimination% versus temperature (°K) (optimum conditions: catalyst dosage= 0.3 g/L, initial concentration= 5 mg/L, contact time= 300 min).

Effect of temperature

In this study, the elimination of chlorpyrifos on the $NiWO_4$ nanoparticles was perused in the temperature range of 298-328°K under pre-determined optimized conditions. The corresponded consequences are illustrated in Fig.10. Fig. 10 clarifies the effect of temperature on the elimination of chlorpyrifos on the $NiWO_4$ adsorbent surface. The elimination of chlorpyrifos on the $NiWO_4$ nanoparticles undergoes decrease as the temperature increases gradually. This is owing to forming bonds between chlorpyrifos and active sites of $NiWO_4$ catalyst being loosed and broken as a result of raising reaction temperature. After those above noted evaluations, the temperature of 298°K considered as an optimized temperature.

Mechanism of the elimination procedure

Considering both obtained data from characterization studies and the adsorption-destruction (elimination) principles represented in the manuscript body, the proposed mechanism (Scheme 1) includes two major steps: 1) adsorption of CP on the surface of synthesized catalyst and 2) destruction of CP by hydrolysis process. To clarify the mechanism, first the metal ions (M) referring to Ni^{2+} and W^{6+} act as electrophiles (Lewis acid sites) coordinate with the sulfur and chlorine atoms and enhances the electrophilic tendency of the phosphorus in center making it more vulnerable to be invaded by H_2O in sequence steps. After adsorption of CP on the surface of $NiWO_4$ nanoparticles, the cleavage of P-O linkages takes place in presence of H_2O molecules (as nucleophiles) whereas the trichloro pyridinol (TCPY) remains on the catalyst surface. Eventually, the diethyl phosphorothioic acid (DEPA) as a destruction product of chloropyrifos separated from the catalyst into the solution (Sarkouhi, *et al.,* 2016).

COCLUSIONS

In this study, for the very first time, the application of synthesized $NiWO_4$ nanoparticles for adsorption-destruction of chloropyrifos (CP) as a widespread organophosphate chemical using in agricultural fields as insecticide was considered and evaluated via the 31P nuclear magnetic resonance (^{31}PNMR). Also, the effects of different operative variables such as catalyst dosage, contact time, initial chlorpyrifos concentration and temperature on the adsorption-destruction efficiency of CP were investigated. Various characterization evaluations proved that the nickel tungstate ($NiWO_4$) nanoparticles synthesized by hydrothermal method were of good and appropriate structural, morphological, crystal size and elemental composition as expected. ^{31}PNMR analysis result data elucidated that CP was successfully eliminated by the catalyst with a yield 100% under optimized conditions of: contact time (300 min), catalyst dose (0.3 g/L), initial pesticide concentration (5 mg/L) and temperature (298°K). Plus, the reaction kinetic data was surveyed utilizing first order model and the values of the rate constant (k) and half-life ($t_{1/2}$) were indicated as 0.0037 1/min and 187.2972 min, respectively. All of the characterization data and experimental results clearly expressed the particular advantageous characteristics of this newly synthesized catalyst for effective adsorption and subsequent destruction of CP as a hazardous chemical. The less toxic diethyl phosphorothioic acid (DEPA) as a main destruction product of chlorpyrifos with synthesized $NiWO_4$ was obtained.

ACKNOWLEDGMENT

The authors give their sincere regards to the Islamic Azad University, Qaemshahr, Iran for all their kindly provided supports.

REFERENCES

Awasthi, M.D.; Prakash, N.B., (1997). Persistence of Chlorpyrifos in Soils Under Different Moisture Regimes. Pestic. Sci., 50 (1): 1–4.

Bavcon Kralj, M.; Trebse, P.; Franko, M., (2007). Applications of Bioanalytical Techniques in Evaluating Advanced Oxidation Processes in Pesticide Degradation. Trends Anal. Chem., 26 (11): 1020–1031.

Benoit-Marqui, F.; Montety, C.; Gilard, V.; Martino, R.; Maurette, M.T.; Maet-Martino, M., (2004). Dechlorvos Degradation studied by 31P-NMR. Environ. Chem. Lett., 2 (2): 93-97.

Carel, W.; van Eijk, E., (1997). Development of Inorganic Scintillators. Nucl. Instrum. Methods Phys. Res. A., 392 (1-3): 285–290.

Cochran, R.C., (2002). Appraisal of Risks from Non-occupational Exposure to Chlorpyrifos. Regul. Toxicol. Pharmacol., 35 (1): 105–121.

De Oliveira, A.L.M.; Ferreira, J.M.; Silva, M. R.S.; de Souza Soraia, C.; Vieira, F.T.G.; Longo, E.; Souza, A.G.; Santos, I. M.G., (2009). Influence of the Thermal Treatment in the Crystallization of $NiWO_4$ and $ZnWO_4$. J. Therm. Anal. Calorim., 97 (167): 167–172.

Dias, A.; Ciminelli, V.S.T., (2001). Thermodynamic Calculations and Modeling of the Hydrothermal Synthesis of Nickel Tungstates. J. Eur. Ceram. Soc., 21(10-11): 2061–2065.

Getzin, L.W., (1981). Degradation of Chlorpyrifos in Soil: Influence of Autoclaving, Soil Moisture and Temperature. J. Econ. Entomo., l74(2): 158–162.

He, H.Y.; Huang, J.F.; Cao, L.Y.; Wu, J.P., (2010). Photodegradation of Methyl Orange Aqueous on $MnWO_4$ Powder under Different Light Resources and Initial pH, Desalination 252 (1-3): 66–70.

Johnson, L.F.; Boyd, G.D.; Nassau, K.; Soden, R.R., (1962). Continuous Operation of a Solidstate Optical Maser. Phys. Rev., 126 (4): 1406–1409.

Lakshmi, C.V.; Kumar, M.; Khanna, S., (2008). Biotransformation of Chlorpyrifos and Bioremediation of Contaminated Soil. Int. Biodeterior. Biodegrad., 62 (2): 204–209.

Mani, S.; Vediyappan, V.; Chen, S.M.; Madhu, R.; Pitchaimani, V.; Chang, J.Y.; Liu, S.B., (2016). Hydrothermal Synthesis of $NiWO_4$ Crystals for High Performance Non-Enzymatic Glucose Biosensors. Sci Rep., 24128: doi: 10.1038/srep24128.

Meiqiang, Y.; Tengcai, M.; Jialiang, Z.; Mingjing, H.; Buzhou, M., (2006). The Effect of Highpressure Arc Discharge Plasma on the Degradation of Chlorpyrifos. Plasm. Sci. Technol., 8 (6): 727–731.

Mori, M.N.; Oikawa, H.; Sampa, M.H.O.; Duarte, C.L., (2006). Degradation of Chlorpyrifos by Ionizing Radiation. J. Radioanal. Nucl. Chem., 270 (1): 99–102.

Pandey, P.S.; Bhave, N.S.; Kharat, R.B., (2006). Structural, Optical, Electrical and Photovoltaic Electrochemical Characterization of $NiWO_4$ Thin Films. Electrochim. Acta., 51(22): 4659–4664.

Penuela, G.A.; Barcelo, D., (1997). Comparative Degradation Kinetics of Chlorpyrifos in Water by Photocatalysis with FeCl2, TiO_2 and Photolysis Using Solid-Phase Disc Extraction Followed by Gas Chromatographic Techniques, Toxicol. Environ. Chem., 62 (1-4): 135–147.

Pullar, R.C.; Farrah, S.; Alford, N. McN., (2007). $MgWO_4$, $ZnWO_4$, $NiWO_4$ and $CoWO_4$ Microwave Dielectric Ceramics. J. Eur. Ceram. Soc., 27 (2-3): 1059–1063.

Quintana-Melgoza, J.M.; Cruz-Reyes, J.; Avalos-Borja, M., (2001). Synthesis and Characterization of $NiWO_4$ Crystals. Mater. Lett., 47 (4-5): 314–318.

Racke, K.D.; Fontaine, D.D.; Yoder, R.N.; Miller, J.R., (1994). Chlorpyrifos Degradation in Soil at Termiticidal Application Rates. Pestic Sci., 42 (1): 43–51.

Ryu, J.H.; Yoon, J.-W.; Lim, C.S.; Shim, K.B., (2006). Microwave-assisted Synthesis of MWO_4 and $MMoO_4$ (M= Ca, Ni) Nano-Powders Using Citrate Complex Precursor. Key Eng. Mater., 317–318: 223–226.

Sadeghi, M.; Yekta, S., (2014). Significance of Chemical Decomposition of Chloroethyl Phenyl Sulfide (CEPS) Using Zinc-Cadmium Oxide (ZnO-CdO) Nanocomposite, Int. J. Bio-Inorg. Hybr. Nanomater., 3 (4): 219-229.

Samet, Y.; Agengui, L.; Abdelhédi, R., (2010). Electrochemical Degradation of Chlorpyrifos Pesticide in Aqueous Solutions by Anodic Oxidation at

Boron-doped Diamond Electrodes. Chem. Eng. J., 161 (1-2): 167-172.

Sarkouhi, M.; Shamsipur, M.; Hassan, J., (2016). Metal Ion Promoted Degradation Mechanism of Chlorpyrifos and Phoxim. Arab. J. Chem., 9 (1): 43-47.

Stephen, D.E.; Timothy, C.W., (2006). Degradation of Chlorpyrifos in Aqueous Chlorine Solutions: Pathways, Kinetics, and Modelling. Environ. Sci. Technol., 40 (2): 546–551.

Singh, R.; Gutch, P.K.; Acharya, J.; Prabha, S., (2011). Detoxification of O,S-diethyl Methyl Phosphonothiolate (OSDEMP), a Simulant of VX, by N,N-dichlorourethane as an Effective Decontaminating Agent. Indian J. Chem., 50 (10): 1504-1509.

Stern, D.L.; Grasselli, R.K., (1997). Propane Oxydehydrogenation Over Metal Tungstates. J. Catal., 167 (2): 570–572.

Song, Z.; Ma, J.; Sun, H.; Wang, W.; Sun, Y.; Sun, L.; Liu, Z.; Gao, C., (2009). Synthesis of $NiWO_4$ Nano-particles in Low-Temperature Molten Salt Medium. Ceram. Int., 35 (7): 2675–2678.

Sundaram, R.; Nagaraja, K.S., (2004). Electrical and Humidity Sensing Properties of Lead (II) Tungstate–Tungsten(VI) Oxide and Zinc(II) Tungstate–Tungsten(VI) Oxide Composites. Mater. Res. Bull., 39 (4-5): 581–590.

Verma, M.; Chandra, R.; Gupta, V. K., (2016a). Synthesis and Characterization of Magnetron Sputtered ZrO_2 Nanoparticles: Decontamination of 2-Choloro Ethyl Ethyl Sulphide and Dimethyl Methyl Phosphonate. J. Environ. Chem. Eng., 4 (1): 219–229.

Verma, M.; Chandra, R.; Gupta, V.K., (2016). Decontamination of 2-Chloro Ethyl Ethyl Sulphide and Dimethyl Methyl Phosphonate from Aqueous Solutions Using Manganese Oxide Nanostructures. J. Mol. Liq., 215 (1): 285-292.

Verma, M.;Gupta, V. K.; Dave, V.; Chandra, R., (2015). Prasad, G.K.; Synthesis of Sputter Deposited CuO Nanoparticles and Their Use for Decontamination of 2-Chloroethyl Ethyl Sulfide (CEES). J. colloid. Interface. Sci., 438(1): 102–109.

Wang, H.; Medina, F.D.; Zhou, Y.D.; Zhang, Q.N., (1992). Temperature Dependence of the Polarized Raman Spectra of $ZnWO_4$ Single Crystals. Phys. Rev. B, 45: 10356–10362.

Whangchai, K.; Uthaibutra, J.; Phiyanalinmat, S.; Pengphol, S.; Nomura, N., (2011). Effect of Ozone Treatment on the Reduction of Chlorpyrifos Residues in Fresh Lychee Fruits. Ozone. Sci. Eng., 33(3): 232-235.

Whitacre, D.M., (2012). Reviews of Environmental Contamination and Toxicology 215. London: Springer New York Dordrecht Heidelberg.

Zhang, Y.; Hou, Y.; Chen, F.; Xia, Z.; Zhang, J.; Hu, X., (2011). The Degradation of Chlorpyrifos and Diazinon in Aqueous Solution by Ultrasonic Irradiation: Effect of Parameters and Degradation Pathway. Chemosphere., 82 (8): 1109-1115.

AUTHOR (S) BIOSKETCHES

Meysam Sadeghi, Instructor, Young Researchers and Elite Club, Ahvaz Branch, Islamic Azad University, Ahvaz, Iran

Sina Yekta, Instructor, Department of Chemistry, Faculty of Basic Sciences, Islamic Azad University, Qaemshahr Branch, Qaemshahr, Iran, *Email: sina.yekta.chem@gmail.com*

Hamed Ghaedi, Assistant Professer, Faculty of Engineering, Bushehr Branch, Islamic Azad University, Bushehr, Iran